Large tetraalkyl ammonium cations produce a reduced conductance state in the sheep cardiac sarcoplasmic reticulum Ca^{2+}-release channel

Andrew Tinker, Allan R. G. Lindsay, and Alan J. Williams
Department of Cardiac Medicine, National Heart and Lung Institute, University of London, London SW3 6LY, United Kingdom

ABSTRACT The purified Ca^{2+}-release/ryanodine receptor channel of the sheep cardiac muscle sarcoplasmic reticulum (SR) functions as a calcium-activated cation-selective channel under voltage clamp conditions following reconstitution into planar phospholipid bilayers. We have investigated the effect of large tetraalkyl ammonium (TAA) cations, $(C_nH_{2n+1})_4N^+$ (n = 4 and 5) on monovalent cation conduction. These cations modify the conductance of the receptor channel at positive holding potentials from the cytosolic side of the channel. Under these conditions, openings are resolved as a mixture of normal full amplitude events and events of reduced conductance. The amplitude of the reduced conductance state is a fixed proportion of the normal open state. As a proportion of all open events, the occurrence of the tetrabutyl ammonium (TBA^+) related subconductance state increases with concentration and increasingly positive holding potential. The TBA^+ related subconductance state displays similar conduction properties to the unmodified channel; with a linear current-voltage relationship, a similar affinity for K^+ and voltage-dependent block by TEA^+. A method was used to quantify the voltage dependence of the occurrence of the TBA^+ effect, which yielded an effective gating charge of 1.66. A second method based on kinetic analysis of the voltage dependence of transitions between the full open state and the TBA^+ related subconductance state produced a similar value. In addition, this analysis revealed that the bulk of the voltage-dependence resided in the off rate. TBA^+ related subconductance events, expressed as a proportion of all open events, saturated with increasing TBA^+ concentration. Kinetic analysis revealed that this could be entirely accounted for by changes in the on rate. Tetrapentyl ammonium ($TPeA^+$) causes a qualitatively similar effect with a subconductance state of lower amplitude. The voltage-dependence of the effect was comparable to that displayed by TBA^+. These findings are interpreted as a form of partial block in which more than one large TAA cation binds at the extremity of the voltage drop to produce an electrostatic barrier for ion translocation.

INTRODUCTION

The use of ions and drugs to block current flow in excitable tissues has been a central theme in electrophysiology. The interaction of a blocker at the single-channel level was first observed by Neher and Steinbach (1) in the acetylcholine receptor-channel. They observed the effects of the charged local anaesthetics QX222 and QX314 on single-channel current fluctuations in chronically denervated frog muscle using the subgigaohm seal patch clamp technique. The normal square pulse like channel openings were broken up into bursts of much shorter openings in the presence of QX222. The conductance of the fully open and closed state were unaffected. Neher and Steinbach suggested the blockers physically plugged the pore while attempting to permeate through the channel. The dwell times of the local anaesthetic within the conduction pathway were observed as the "flicker" in the open channel current. This kind of behavior has been observed in a variety of other single-channel studies, e.g., with decamethonium in the sarcoplasmic reticulum (SR) K^+ channel (2) and large conductance Ca^{2+}-activated K^+ channel (3) and it is now accepted as a common motif of channel block.

Recently, other forms of channel blockade have emerged. Protons in the dihydropyridine- (DHP) sensitive calcium channel (4–6) and Zn^{2+} in voltage-dependent sodium channels of cardiac muscle (7, 8) induce a rapid switching between the normal full open channel conductance level and one with a reduced but nonzero conductance. This behavior has been interpreted as a "blocker"-induced conformational change rather than entry of the blocking ion into the conduction pathway of the channel. In this paper we present evidence for a form of partial block by tetrabutyl ammonium (TBA^+) and tetrapentryl ammonium ($TPeA^+$) in the sheep cardiac ryanodine receptor channel.

Address correspondence to Dr. Williams.

METHODS

Materials

Phosphatidyl-ethanolamine was purchased from Avanti Polar Lipids, Inc. (Birmingham, AL). and Phosphatidyl-choline from Sigma Chemical Co. (St. Louis, MO). [^{3}H]-ryanodine was obtained from New

0006-3495/92/05/1122/11 $2.00

England Nuclear Ltd. (DuPont UK Ltd., Stevenage, Herts, UK). Aqueous counting scintillant was purchased from Amersham International. All quaternary ammonium compounds were bought from Aldrich Ltd and all other chemicals from BDH Ltd or Sigma. Tetrabutyl ammonium (TBA^+) and tetrapentyl ammonium ($TPeA^+$) were bought as bromide salts. Tetraethyl ammonium (TEA^+) was obtained as a chloride salt.

Preparation of the purified sheep cardiac ryanodine receptor channel

The purified sheep cardiac ryanodine receptor-channel was isolated and incorporated into liposomes as previously described (9).

Planar lipid bilayer methods

Conduction studies were carried out using essentially uncharged bilayers, formed from suspensions of phosphatidylethanolamine in decane (35 mg/ml). Bilayers were formed across a 200-μm diameter hole in a polystyrene partition which separated two chambers referred to as the *cis* (vol 0.5 ml) and *trans* (vol 1.5 ml) chambers. The *trans* chamber was held at virtual ground whereas the *cis* chamber could be clamped at various holding potentials relative to ground. Current flow across the bilayer was measured using an operational amplifier as a current-voltage converter as described by Miller (10). Bilayers were formed in solutions of 200 mM KCl, 20 mM HEPES, KOH to pH 7.4 resulting in a solution of 210 mM K^+. An osmotic gradient was established by the addition of a small quantity (usually 50 to 100 μl) of 3 M KCl to the *cis* chamber. Proteo-liposomes were added to the *cis* chamber and stirred. To induce fusion of the vesicles with the bilayer a second small aliquot (50–100 μl) of 3 M KCl was added to the *cis* chamber. After incorporation, further fusion was prevented by perfusion of the *cis* chamber with 200 mM KCl, 20 mM HEPES, KOH to pH 7.4. Solutions contained 10 μM contaminant free Ca^{2+} which was sufficient for channel activation. Experiments were carried out at room temperature (21 ± 2°C).

Single-channel data acquisition and analysis

Single-channel current fluctuations were displayed on an oscilloscope and recorded on videotape. When analyzed, data were filtered using an eight pole Bessel filter (Frequency Devices 902, Lyons Instruments, Herts., UK) at 1.0 to 4.0 kHz and digitized at 2.0–8.0 kHz using an AT based system (Intracel, Cambridge UK). Single-channel current amplitudes were measured from digitized data using manually controlled cursors. The representative traces shown in the figures were displayed on a Hewlett Packard 7475A plotter following digitization using a PDP 11/73 based system (Indec, Sunnyvale, CA).

To measure single-channel current amplitudes data were filtered at 1 kHz and digitized at 4 kHz. The addition of TBA^+ leads to the production of a reduced conductance level associated with the normal fully open current amplitude. The effect of TBA^+ on the single-channel current is shown in Fig. 1. In such records, two measurements of current amplitude were made. The first is a measurement of the supposed full conductance event, i.e., the current amplitude between level 0 and level 2 in Fig. 1. The other is a measurement of the reduced conductance event, the effect attributed to TBA^+, i.e., between level 0 and level 1.

Two methods were used to examine the concentration and voltage-dependence of the occurrence of the TBA^+ related subconductance state. In the first, a method was devised to calculate the fraction of TBA^+ related subconductance events as a proportion of total open events. The second analyzed the kinetics of transition between the fully open (level 2 in Fig. 1) and TBA^+ related subconductance state (level 1 in Fig. 1).

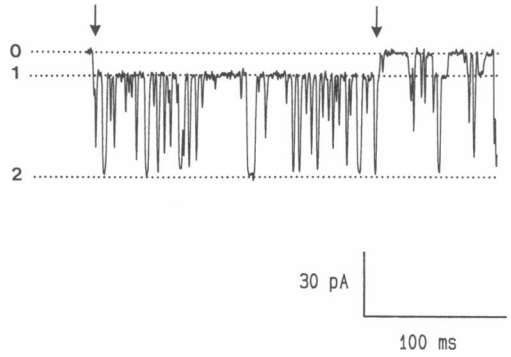

FIGURE 1 Representative single-channel current fluctuations at a holding potential of 60 mV with 100 μM TBA^+ present in the *cis* and *trans* chambers (filtered at 1 kHz). Level 0 corresponds to the closed level, level 1 to the TBA^+ related subconductance state and level 2 to the fully open state. The arrows indicate a long opening of the kind used for the kinetic analysis.

In the first method, a run of 5–10 s of data at a particular voltage and concentration of TBA^+ was filtered at 1 kHz and digitised at 4 kHz. Such runs displayed only a single active channel. Open and closed lifteime files were compiled using a 50% amplitude detection threshold with the cursors set manually on the fully open level (level 2 in Fig. 1) and the closed level (level 0 in Fig. 1). Events above the threshold were considered to be full open events and those below closed events. The files yielded a mean open and closed time and these could be used to calculate the probability of occurrence of the fully open event (P_o). Additional open and closed lifetime files were compiled on exactly the same piece of data. On this occasion the cursors were set on the subconductance level (level 1 in Fig. 1) and the closed level (level 0 in Fig. 1) and lifetimes again assessed using a 50% amplitude threshold. Visual inspection of the analyzed record revealed that with 1 kHz filtering the TBA^+ related subconductance state events were readily distinguished from baseline noise even at low positive voltages. These files could then be used to estimate the probability of all open events (P_{tot}), i.e., fully open events and TBA^+ related subconductance state events. The probability of occurrence of the subconductance events (P_s) is given by $P_{tot} - P_o$. Two major parameters are used in the results section; the ratio ($R_{s/o}$) of the occurrence of the TBA^+ related subconductance state to fully open events, i.e., P_s/P_O and the fraction (F_s) of total open events occurring as the TBA^+ related subconductance state, i.e., $100.P_s/P_{tot}$.

In the second method it was assumed that the transition between the fully open (level 2 in Fig. 1) and the TBA^+ related subconductance state (level 1 in Fig. 1) represented the entry and exit of TBA^+ into and out of the conduction pathway. Information on the kinetics of TBA^+'s interaction was obtained by lifetime analysis. The data were filtered at 4 kHz and digitized at 8 kHz. As in the previous method, sections of data with only a single active channel in the record were chosen. Pieces of this record were selected in which the channel was open (in level 1 or 2 in Fig. 1) for a prolonged period, for example between the arrows in Fig. 1. In general, a single piece of data contained at least 20 transitions. Manually controlled cursors were fitted to the two levels and a discriminator was set halfway between the two current amplitudes. Points above and below this level represent dwell times spent at the fully open state and the TBA^+ related subconductance state

respectively. Large numbers of such pieces of data were needed to compile over 500 events. Low pass filtering at 4 kHz did not allow us to fully resolve events of duration <0.18 ms and such events were removed from the file. In general, lifetimes were calculated on stripped files containing between 500 and 1,500 transitions. We followed the methods of Colquhoun and Sigworth (11) in fitting lifetimes to probability density functions. The lifetime files were stripped with a t_{min} of 0.18 ms and a t_{max} of 64,000 ms. Stripping resulted in removal of less than 20% of events. These lifetimes were fitted to probability density functions with one or two exponential terms optimizing the variables to maximize the fit using a simplex algorithm. The adequacy of fit is expressed as a $\log_e$ (likelihood). A missed events correction was used as described by Colquhoun and Sigworth (11). The fit to one and two exponential terms was assessed by eye and by testing twice the difference in $\log_e$ (likelihood) against a chi-squared distribution at the 1% level with the relevant degrees of freedom. Both open and TBA^+ related subconductance state lifetime files were found to be adequately described by probability density functions with a single exponential term.

$TPeA^+$ causes a qualitatively similar effect to TBA^+ and a similar method of analysis was used to calculate the current amplitudes and voltage-dependence of the effect. 1 kHz filtering was adequate to distinguish the $TPeA^+$ related subconductance state from the baseline noise. 4 kHz filtering was used to examine the kinetics of transition between the fully open state (level 2 in Fig.. 11 *a*) and the $TPeA^+$ related subconductance state (level 1 in Fig. 11 *a*).

RESULTS

We have established that the purified sheep cardiac muscle SR ryanodine receptor protein functions as a ligand-sensitive cation-selective channel when reconstituted into planar lipid bilayers and displays properties consistent with a role as the SR Ca^{2+}-release channel (9). In the absence of divalent cations the channel has been shown to have a high conductance with monovalent cations (12). In symmetrical 210 mM K^+ the current-voltage relationship of the receptor-channel is linear over the voltage range −80 mV to 80 mV and the mean conductance was 759 ± 3 pS (±S.E.M., n = 13).

TBA^+ effect

The effect of TBA^+ is illustrated in Fig. 2. TBA^+ was added as small aliquots from concentrated stock solutions to both the *cis* and the *trans* chambers. The appearance of the TBA^+ related subconductance state is predictable and the proportion of the total open time spent in the TBA^+ related subconductance state (F_s) is fixed within experimental error. For example with 100 μM TBA^+ at a holding potential of +60 mV the proportion is 59.5 ± 3.9% (±S.E.M., n = 8). This value was independent of total P_o implying that the TBA^+ related subconductance state does not represent the chance superposition of another channel of reduced conductance.

The occurrence of the TBA^+ related subconductance state is both voltage- and concentration-dependent. The TBA^+ related subconductance state is not present at negative voltages but becomes more evident as the holding potential becomes increasingly positive (Fig. 3 *a*). Additionally, at a fixed holding potential it becomes increasingly obvious as the concentration of TBA^+ is increased (Fig. 3 *b*). The effect can be detected at 100 mV with as little as 5 μM TBA^+ present symmetrically. The normal channel openings are unaffected in amplitude with up to 500 μM TBA^+. However, with higher

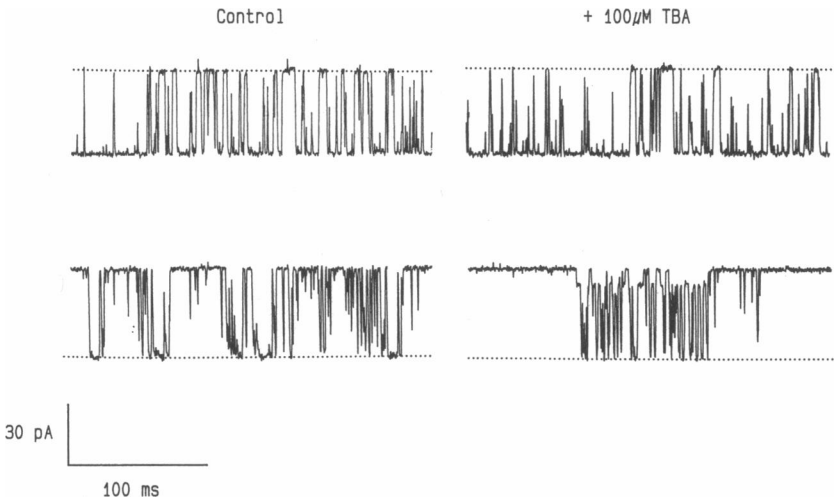

FIGURE 2 Representative single-channel current fluctuations at holding potentials of ±60 mV. The upper traces are at −60 mV and the lower at 60 mV. The control traces are shown in the left panel and those following the addition of 100 μM TBA^+ to the *cis* and *trans* chambers in the right panel. Open channel current levels are indicated by the dotted lines.

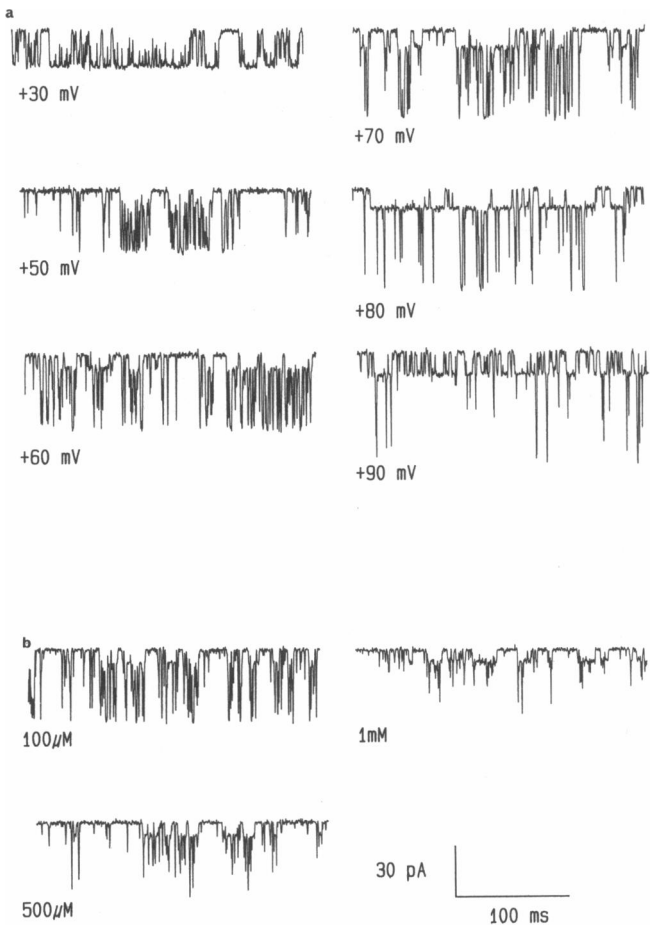

FIGURE 3 (*a*) Representative single-channel current fluctuations at a series of holding potentials (as indicated in the figure) following the addition of 100 μM TBA^+. Downward deflection of the current trace is the channel opening. The TBA^+ related subconductance state (see Fig. 1) becomes increasingly obvious as the holding potential is increased. (*b*) Representative single-channel current fluctuations at a holding potential of 60 mV. Downward deflection of the current trace is the channel opening. The traces were recorded with increasing concentrations of TBA^+ (as indicated in the figure). The TBA^+ related subconductance state (see Fig. 1) becomes increasingly obvious as the concentration of TBA^+ is increased.

concentrations of TBA^+ at positive holding potentials opening events rarely reach the fully open level.

The effect induced by TBA^+ is reversed when the cation is perfused out with 210 mM K^+ from the *cis* chamber. This confirms that TBA^+ is only effective from the cytosolic face of the channel protein. In all subsequent experiments despite the asymmetry of the effect with the large TAA cations, the data is analyzed with them present in both *cis* and *trans* chambers to avoid the possible effect of asymmetric surface charges caused by binding of TBA^+ or $TPeA^+$ to the bilayer (2).

Nature of the TBA^+ related subconductance state

The properties of the TBA^+ related subconductance state were investigated. The current amplitude of the TBA^+ related subconductance state was measured at 5 mV steps upwards from a voltage at which the TBA^+ related subconductance state could be clearly identified. Investigations were performed with a range of TBA^+ concentrations. The current-voltage relationship for the reduced conductance state was linear over the voltage range studied (30 to 100 mV). The conductance was calculated from the slope of the least squares linear regression and gave a mean value of 163 ± 9.9 pS (±S.E.M., $n = 7$). Alternatively this may be expressed as a percentage of the control conductance, in which case it gives a value of ~21%. An example of the current-voltage relationship is shown in Fig. 4. The current amplitude at a given voltage was independent of TBA^+ concentration.

With K^+ as the permeant ion, the conductance-activity relationship of the purified sheep cardiac ryanodine receptor-channel follows Michaelis-Menten type kinetics with a maximal conductance of 900 pS and a K_m of 19.9 mM (12). The TBA^+ related subconductance state displays similar behavior. At a series of K^+ concentrations from 100 mM to 600 mM the ratio of the TBA^+ related subconductance state current amplitude to the fully open channel current at any particular voltage was constant with 100 μM TBA^+ (data not shown). The above suggests that the affinities for K^+ of the TBA^+ related subconductance state and the unmodified channel are similar.

The purified ryanodine receptor-channel is blocked in

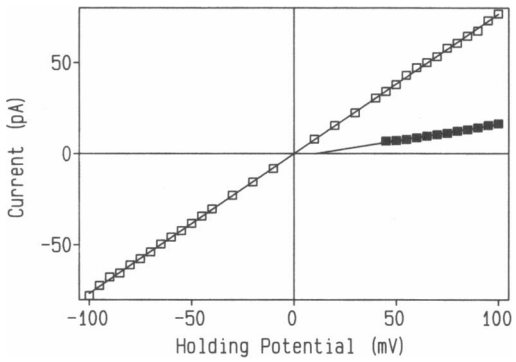

FIGURE 4 Single channel current-voltage relationships obtained for the full conductance state in symmetrical 210 mM K^+ and for the TBA^+ related subconductance state with 100 μM TBA^+ present in *cis* and *trans* chambers. (□: control full conductance state, ■: TBA^+ related subconductance state). Conductance values are quoted in the text.

a voltage-dependent fashion by TEA^+ (12). The TBA^+ related subconductance state is likewise blocked. After the addition of a high concentration of TBA^+ (500 μM or 1 mM TBA^+) a current-voltage relationship was obtained for the TBA^+ related subconductance state. 20 mM TEA^+ was then added symmetrically and a further current-voltage relationship was obtained. There was a reduction in TBA^+ related subconductance current amplitude in the presence of TEA^+ and the relative conductance decreased as the holding potential became increasingly positive. Subsequent analysis using a Woodhull (13) model led to an effective valence of block of 0.89 ± 0.03 and a $K_b(0)$ of 410 ± 11 mM (±S.E.M., $n = 3$). The effective valence of block is similar to that seen in the unmodified channel suggesting that TEA^+ has access to its normal site (12). This is illustrated in Fig. 5.

Simple kinetic scheme is used as a basis for analysis

A simple kinetic scheme was used as a framework for analysis. To reduce the complexity of the state diagram TBA^+ was assumed to only interact with the open channel. This seems reasonable as direct openings to and closures from the TBA^+ related subconductance state are an uncommon event (Figs. 1 and 2) under conditions where full openings within a burst are well resolved, i.e., at low TBA^+ concentrations and positive holding potentials within the range 40–75 mV. At higher TBA^+ concentrations and higher positive voltages, openings do occur more commonly directly to the TBA^+ related subconductance state (e.g., Fig. 3), although these are the conditions where full openings are most attenuated.

The rate constant for transition between the fully open and TBA^+ related subconductance state (K_{on}) is calculated from the distribution of the open times and the rate constant for the reverse reaction (K_{off}) from the distribution of TBA^+ related subconductance state lifetimes (see below).

$$\text{CLOSED} \rightleftharpoons \text{OPEN} \underset{K_{off}}{\overset{K_{on}}{\rightleftharpoons}} \text{TBA.SUBCONDUCTANCE STATE}$$

SCHEME 1

If the second equilibrium is determined by the Boltzmann distribution then the ratio of the TBA^+ related subconductance state to the fully open state ($R_{s/o}$) is given by

$$R_{s/o} = \exp\left[(z_{tot}FV - Gi)/RT\right], \quad (1)$$

and in a linearized form

$$Ln\left[R_{s/o}\right] = z_{tot}F/RT.V - Gi/RT, \quad (2)$$

where z_{tot} is the equivalent gating charge (the total voltage-dependence of the effect), V is the membrane potential and R, T, and F have their usual meanings. The term Gi/RT reflects the equilibrium of the reaction at zero membrane potential. The value of RT/F used was 25.2 mV at 20°C.

K_{on} and K_{off} are derived from the time constants used in the probability density functions to describe the dwell times in the full open and TBA^+ related subconductance state within an opening.

$$\tau_{on}^{-1} = K_{on} = [\text{TBA}].K'_{on} \quad (3)$$

$$\tau_{off}^{-1} = K_{off}. \quad (4)$$

This simple scheme predicts that K_{on} should vary linearly with concentration and K_{off} should be independent of it. K'_{on} is the absolute association rate constant. F_s, the fraction of total open events occurring as TBA^+ related subconductance events, will obey Michaelis-Menten type kinetics with increasing TBA^+ concentration.

In addition, if the rate constants are voltage dependent and follow the Boltzmann distribution then they will be described by:

$$K_{on}(V) = K_{on}(0).\exp\left[z_{on}FV/RT\right] \quad (5)$$

$$K_{off}(V) = K_{off}(0).\exp\left[-z_{off}FV/RT\right], \quad (6)$$

where $K(V)$ is the rate constant at a particular voltage, $K(0)$ is the rate constant at 0 mV and z is the effective gating charge for the respective reaction.

Plots of the natural logarithm of K_{on} and K_{off} against voltage should be linear with slope $z_{on}F/RT$ and $-z_{off}F/RT$ and intercept Ln $[K_{on}(0)]$ and Ln $[K_{off}(0)]$,

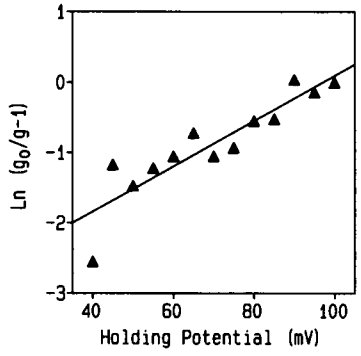

FIGURE 5 The linearized plot of the Woodhull model for voltage-dependent block by 20 mM TEA^+ of the TBA^+ related subconductance state in the presence of 1 mM TBA^+ ($r = 0.9$). g/g_0 is the relative conductance. Parameters are quoted in the text.

respectively. In addition, the total voltage-dependence (z_{tot}) of the effect will be given by $z_{on} + z_{off}$. When fits to this scheme are given the units for rate constants are ms^{-1} and concentration μM except if stated to the contrary.

Occurrence of the TBA⁺ effect is voltage dependent and follows the Boltzmann distribution

A series of experiments were performed to calculate the ratio of TBA⁺ related subconductance events to fully open events ($R_{s/o}$) at various holding potentials with three concentrations of TBA⁺. The data fit the Boltzmann distribution well and the curves for the three concentrations are similar in slope but have different intercepts (the data for two of those concentrations are shown in Fig. 6). The mean slope for all concentrations was 0.066 ± 0.004, corresponding to an equivalent gating charge of 1.66 ± 0.10 (±S.E.M., n = 8). The intercept, the value of which is an expression of the equilibrium of the reaction at 0 mV, for 100 μM TBA⁺ was −3.27 ± 0.49 (±S.E.M., n = 5).

Concentration-dependence of the TBA⁺ effect

The concentration of TBA⁺ was varied by aliquoting small quantities of a concentrated stock solution into the *cis* and *trans* chambers. F_s was calculated at a series of concentrations varying between 50 and 500 μM at a holding potential of 60 mV. The results fit Michaelis-Menten type kinetics with a V_{max} close to one (0.91 ± 0.02, ±S.E.M., n = 5) and a K_m of 45 ± 7 μM at 60 mV (±S.E.M., n = 5). An example of an Eadie-Hoftsee plot is shown in Fig. 7.

Analysis of the kinetics of the TBA⁺ effect

In some runs of recording, the channel was particularly active and a large proportion of the trace was occupied by transitions between the fully open (level 2 in Fig. 1) and TBA⁺ related subconductance state (level 1 in Fig. 1). Using such pieces of data, it is possible to obtain kinetic information about these transitions (see methods). The data in over 90 lifetime files fitted probability density functions with single exponential time constants for both open and TBA⁺ related subconductance state lifetime distributions (Fig. 8). The reciprocal of the time constant in such distributions corresponds to the rate constant.

The voltage-dependence of K_{on} and K_{off} was studied in four experiments with 100 μM TBA⁺ at a series of five or more holding potentials between 50 and 80 mV. The natural logarithm of the rate constants were plotted against the holding potential (Fig. 9). For both K_{on} and K_{off} such plots were linear, fitting the model detailed above. $K_{off}(V)$ can be best fitted by z_{off} = 1.34 ± 0.09 and $Ln\ [K_{off}(0)]$ = 3.09 ± 0.27 (K_{on} = 22.0 ms^{-1}) (±S.E.M., n = 4). $K_{on}(V)$ can best be fitted by z_{on} = 0.47 ± .05 and $Ln[K_{on}(0)]$ = −1.02 ± 0.12 (K_{off} = 0.36 ms^{-1}) (±S.E.M., n = 4). Thus, K_{off} is approximately three times more voltage-dependent than K_{on}. In addition, the total voltage dependence of the reaction is best

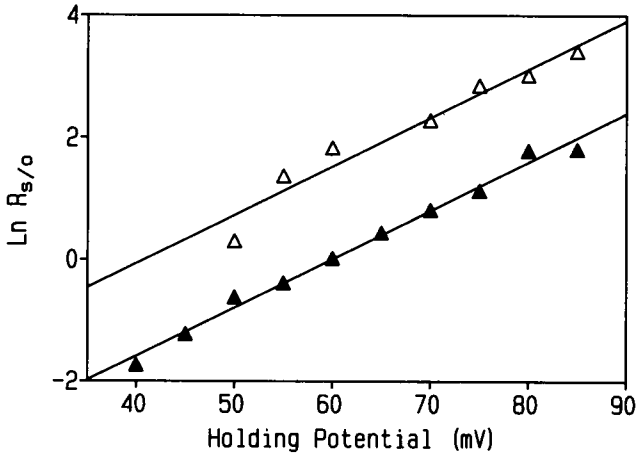

FIGURE 6 A plot of the natural logarithm of $R_{s/o}$ against holding potential with 100 μM TBA⁺ (▲, r = 0.99) and 500 μM TBA⁺ (△, r = 0.95) present in the *cis* and *trans* chambers.

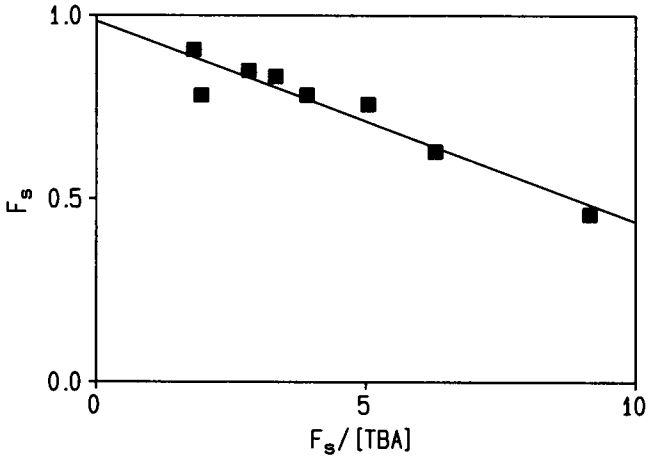

FIGURE 7 An Eadie-Hoftsee plot showing the concentration dependence of the occurrence of the TBA⁺ related subconductance state at a holding potential of 60 mV (r = −0.95). TBA⁺ concentration is quoted in mM.

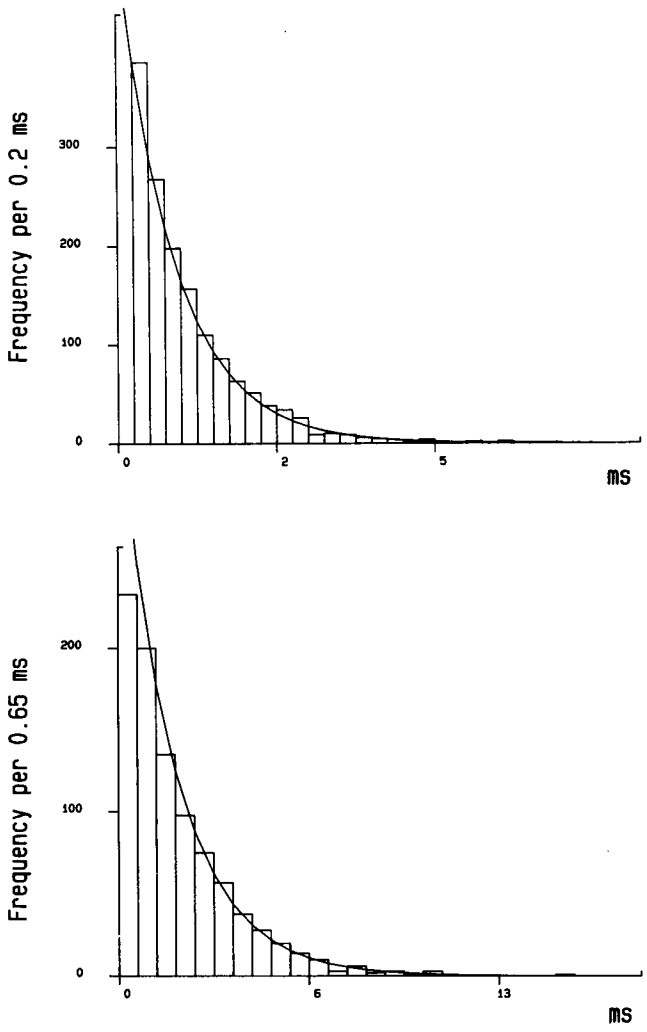

FIGURE 8 Dwell time histograms in the presence of 100 μM TBA^+. The upper panel shows full open state lifetimes at a holding potential of 55 mV and the lower panel shows TBA^+ related subconductance state lifetimes at a holding potential of 70 mV. The solid line is the probability density function with a single exponential with tau = 0.88 ms in the upper panel and tau = 1.86 ms in the lower panel.

described by an effective gating charge of 1.81 agreeing closely with the value determined from the slope of the plot of the natural logarithm of $R_{s/o}$ against holding potential (Fig. 6).

In the simple kinetic scheme outlined above, K_{on} should increase linearly with increasing TBA^+ concentration and K_{off} should be independent of it. The concentration dependence was investigated in four experiments at a holding potential of 60 mV by increasing the TBA^+ concentration in steps over a range of 40 to 500 μM. One such experiment is shown in Fig. 10. It is apparent that K_{on} increases dramatically and linearly with TBA^+ concentration. K_{off} is less dependent on concentration,

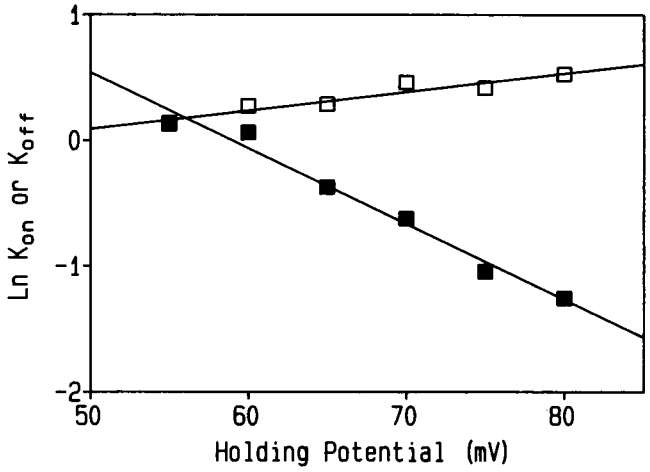

FIGURE 9 The voltage-dependence of K_{on} and K_{off} with 100 μM TBA^+ present in the *cis* and *trans* chambers. The solid lines indicate the least squares linear regression lines, with parameters as given in the text, for the natural logarithm of K_{on} (□, $r = 0.95$) and K_{off} (■, $r = -0.99$) against holding potential. K_{on} and K_{off} have a similar value at a holding potential of 55 mV and is indicated by a single filled square.

the ratio of slopes of K_{on} to K_{off} of the least squares linear regression lines was 13.5 ± 2 (±S.E.M., $n = 4$). The concentration-dependence of K_{on} is given by 8.9 ± 1.2E − 3.[TBA] + 0.59 ± .14 ms^{-1} (±S.E.M., $n = 4$). Within our experimental error K_{off} is very likely to be independent of TBA^+ concentration. In none of the four experiments was the correlation coefficient of K_{off} versus TBA^+ concentration significantly different from $r = 0$

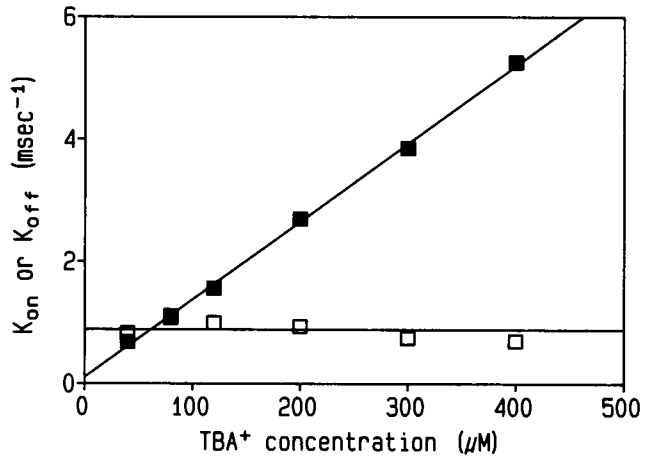

FIGURE 10 The concentration dependence of K_{on} and K_{off} for TBA^+ at a holding potential of 60 mV. The least squares linear regression line through the filled squares indicates the concentration dependence of K_{on} ($r = 1.0$). The second line is a horizontal line based on the assumption that K_{off} (□) is independent of TBA^+ concentration.

when tested at the 5% level and if the results are pooled this is still the case ($r = -0.17, n = 23$). This result gives an explanation for the reduction in fully open current amplitude seen at higher TBA^+ concentrations; K_{on} becomes so fast that the fully open current amplitude is attenuated.

Effect of tetrapentyl ammonium

$TPeA^+$ causes a qualitatively similar effect to TBA^+ (Fig. 11 *a*). The effect is apparent at a holding potential of 100 mV with 10 μM $TPeA^+$. The current amplitude of the $TPeA^+$ related subconductance state at a given voltage is smaller than that observed with TBA^+. Full conductance events were unaffected in amplitude even with high concentrations of $TPeA^+$ and at high positive holding potentials. The current-voltage relationship of the $TPeA^+$ subconductance state was linear and had a mean value of 102 pS ±5.7 (±S.E.M., $n = 5$). This corresponds to ~14% of the control conductance (Fig. 11 *b*).

The voltage-dependence of the $TPeA^+$ effect was investigated using the approach described for TBA^+. The dependence of the occurrence of the $TPeA^+$ related subconductance state on voltage followed the Boltzmann distribution with a slope of 0.068 ± 0.009 (±S.E.M., $n = 4$) corresponding to an effective gating charge of 1.71 ± 0.22 (Fig. 12 *a*), which is similar to that obtained with TBA^+.

The kinetics of $TPeA^+$ interaction with the channel were slower than those of TBA^+ (compare Figs. 9 and 12 *b* at a given voltage). This meant that sufficient data to compile lifetime histograms was difficult to obtain. One experiment with 100 μM $TPeA^+$ is shown in Fig. 12 *b*. As for TBA^+ both lifetime histograms were best described by probability density functions with a single exponential. The effect of voltage on K_{on} and K_{off} was examined. $K_{on}(V)$ is best described by $z_{on} = 0.4$ and $Ln[K_{on}(0)] = -1.9$ ($K_{on} = 0.15\ ms^{-1}$) and $K_{off}(V)$ by $z_{off} = 1.49$ and $Ln[K_{off}(0)] = 9.86$ ($K_{off} = 1.9E4\ ms^{-1}$). The pattern is similar to that of TBA^+ with K_{off} accounting for the greater proportion of the voltage-dependence (Fig. 12 *b*).

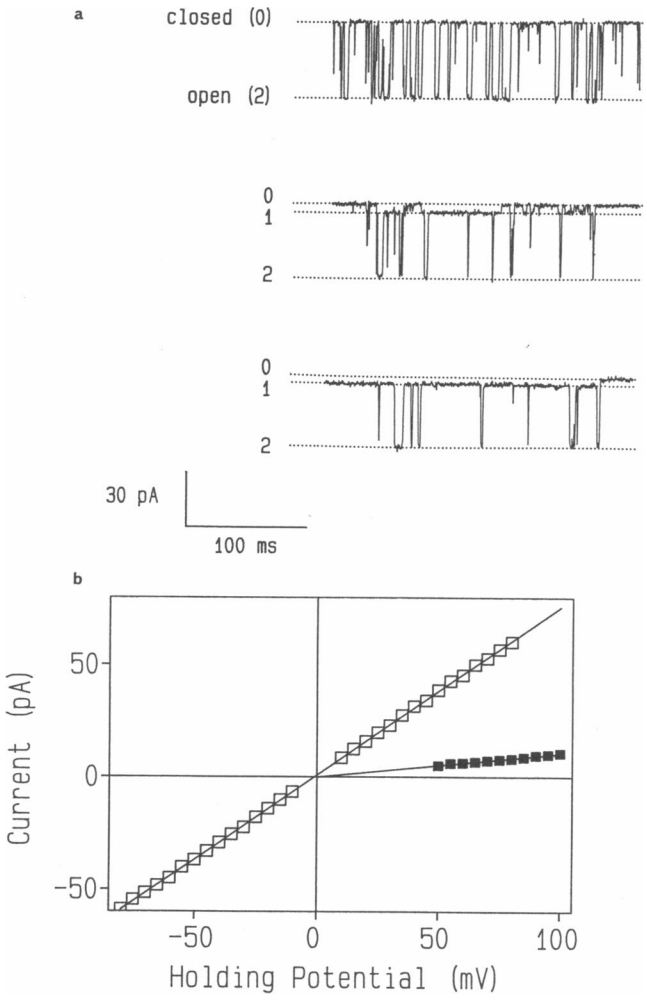

FIGURE 11 (*a*) Representative single-channel current fluctuations at a holding potential of 60 mV. The upper trace is the control trace. The middle trace and lower trace indicate the effect of adding 100 μM $TPeA^+$. The P_o was considerably higher in the lower as compared to the middle trace and the bulk of the trace shows the interaction of $TPeA^+$ with the open channel. The closed and open level is indicated by the dotted lines labeled 0 and 2 respectively. The level of the $TPeA^+$ related subconductance state is indicated by the dotted line labeled 1. (*b*) Single-channel current-voltage relationships obtained for the full conductance state in symmetrical 210 mM K^+ and for the $TPeA^+$ related subconductance state following the addition of 100 μM $TPeA^+$ to the *cis* and *trans* chambers. (□; control full conductance state, ■-$TPeA^+$ related subconductance state). Conductance values are as quoted in the text.

DISCUSSION

Do TBA^+ and $TPeA^+$ enter the conduction pathway?

The addition of either TBA^+ or $TPeA^+$, rather than producing a complete cessation of current flow, leads to a state of reduced conductance. An apparently similar form of block has been observed in other channels. Pietrobon, Prod'hom and Hess (5) observed in single L-type calcium channels with monovalent cations as the charge carrier that decreasing pH led to the production of a reduced conductance state. A similar phenomenon was reported to be caused by Zn^{2+} in the voltage-activated sodium channel of canine cardiac muscle sarcolemma (8). In both these studies, a model was

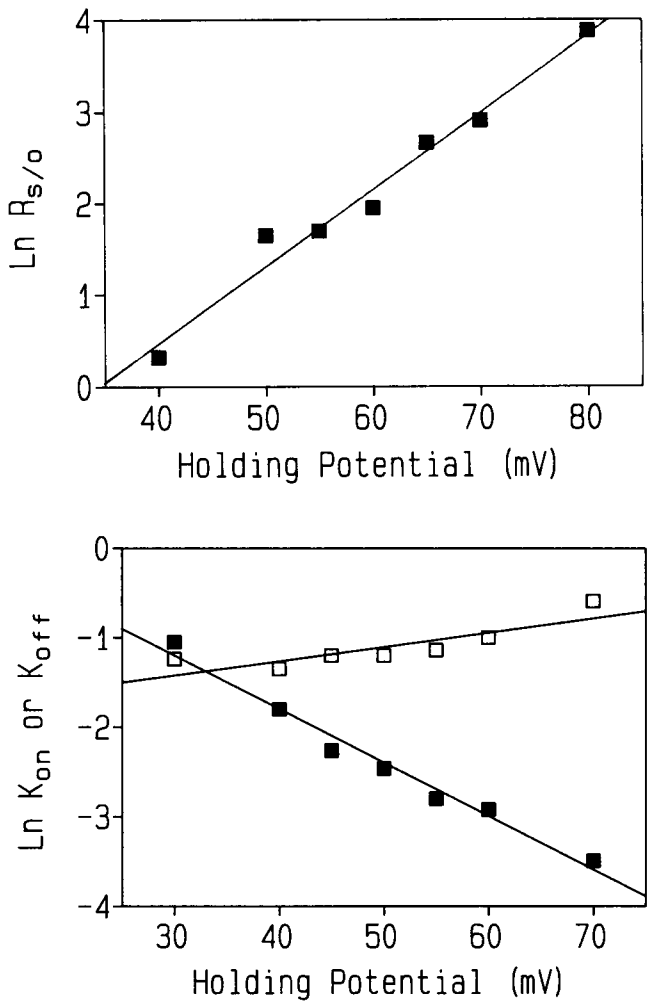

FIGURE 12 (*a*) A plot of the natural logarithm of $R_{S/O}$ against holding potential following the addition of 100 μM $TPeA^+$ to the *cis* and *trans* chambers. (■, $r = 0.98$). Values are as quoted in the text. (*b*) The voltage-dependence of K_{on} and K_{off} with 100 μM $TPeA^+$ present in the *cis* and *trans* chambers. The solid lines indicate the least squares linear regression lines for the natural logarithm of K_{on} (□, $r = 0.85$) and K_{off} (■, $r = -0.99$) against holding potential. The parameters as given in the text.

proposed in which the conductance change was represented by a conformationl change in the protein. The key kinetic argument was that K_{off} was dependent on the "blocker" concentration and thus simpler schemes would not suffice.

If we apply similar kinetic arguments (see Scheme 2), how might such an explanation be invoked to explain TBA^+'s effect on the ryanodine receptor-channel? TBA^+ would bind to a single site outside the voltage drop. The binding would favor a highly voltage-dependent transition between the normal fully open state and a reduced conductance state. Binding and unbinding of TBA^+ could occur from either state and the transition would occur, albeit rarely, in the absence of TBA^+.

CLOSED ⇌ OPEN ⇌ SUBCONDUCTANCE STATE
⇅ ⇅
TBA.OPEN ⇌ TBA.SUBCONDUCTANCE STATE

SCHEME 2

Such a kinetic scheme is highly flexible and has some attractive features. The effective gating charge of TBA^+ lies in the range of 1.66 to 1.81. The supposition that the transition between the subconductance state and fully open state is highly voltage-dependent removes the problem of moving so many large positively charged ions into the conduction pathway and yet still allowing K^+ current to flow.

In the ryanodine receptor-channel the data are consistent with TBA^+ interacting at a single site. K_{on} is proportional to TBA^+ concentration while K_{off} is independent of it. It is thus possible to propose a limiting case of Scheme 2 in which the subconductance state is only present in the presence of TBA^+. As in Scheme 2 the transition between TBA.OPEN and the SUBCONDUCTANCE STATE is highly voltage-dependent and much faster than the binding reaction. The dwell-time histograms will then be adequately described by single exponentials. With these limitations, this scheme will qualitatively reproduce TBA^+'s behavior.

Does this scheme explain the effect of $TPeA^+$?

We have no way of disproving Scheme 2 or simpler versions thereof. The action of TBA^+ and $TPeA^+$ are qualitatively similar and additionally the net voltage-dependence of their effects is the same. However there are some important quantitative differences. In the first instance $TPeA^+$'s kinetics are different from those of TBA^+ but this might arise if the binding site is relatively hydrophobic resulting in different dwell times. The second problem is that the conductance of the $TPeA^+$ related subconductance state is obviously different from that seen with TBA^+. One solution to this problem is to postulate that $TPeA^+$ induces a different conformational change to that of TBA^+ resulting in a state with a different and lower conductance. In other words, to explain the action of both TBA^+ and $TPeA^+$ we would need to propose the unlikely possibility of two distinct kinetic schemes, one for each species.

The alternative explanation is that both TBA^+ and $TPeA^+$ interact directly with the conduction pathway leading to a form of partial block. This possibility is not without precedent as it has been used to explain the

appearance of a subconductance state in the acetylcholine receptor in the presence of curare (14).

Possible kinetic scheme

The results were analyzed in terms of a very simple scheme (Scheme 1). The interaction of a single TBA^+ with the open channel to produce the effect explained much of the data. Unfortunately, the voltage-dependence of the effect suggests that at least two and probably more TBA^+s or $TPeA^+$s must enter the conduction pathway to explain the effect. For the sake of argument it is assumed that four TBA^+s or $TPeA^+$s must enter to induce the subconductance state and that only on the addition of the fourth cation is the effect produced. A possible kinetic scheme, using TBA^+ as an example, is

$$\text{CLOSED} \rightleftharpoons \text{OPEN} \underset{k_{-1}}{\overset{k_1}{\rightleftharpoons}} TBA_1O \underset{k_{-2}}{\overset{k_2}{\rightleftharpoons}} TBA_2O$$

$$\underset{k_{-3}}{\overset{k_3}{\rightleftharpoons}} TBA_3O \underset{K_{off}}{\overset{K'_{on}}{\rightleftharpoons}} TBA_4\text{SUBCONDUCTANCE}.$$

SCHEME 3

In Scheme 3, the first three time constants are suggested to be so fast that the measured K_{on} approximates to the one shown in the diagram i.e. $K'_{on} \ll k_1$, k_2, and k_3. The first three TBA^+s bind relatively easily, and at relatively low TBA^+ concentrations and holding potentials greater than 40 mV, the probability is high that a single channel is in the kinetic state TBA_3O. The addition of the fourth TBA^+ does not occur until higher concentrations, i.e., k_1/k_{-1}, k_2/k_{-2} and $k_3/k_{-3} \gg K'_{on}/K_{off}$.

Scheme 3 successfully explains the total voltage-dependence of the effect. In addition, lifetime histograms for the dwell times in each of the states will be adequately described by probability density functions with a single exponential term. However, K_{off} is considerably more voltage-dependent than K_{on}. One possible explanation is that to return to the fully open state more than one TBA^+ needs to unbind.

The concentration-dependence of the effect presents a problem for this kind of model. There ought to be some degree of positive cooperativity in the appearance of the effect as measured by F_s; instead of which TBA^+ behaves as if it binds to a single site. The limitations we have placed on the rate constants in Scheme 3 would only let positive cooperativity occur at low concentrations, perhaps lower than examined experimentally. In effect, the concentration-dependence would then obey Michaelis-Menten type kinetics and K_{on} would depend linearly on concentration and K_{off} would be independent of it. It is interesting to note that the averaged linear regression line for the concentration-dependence of K_{on} intersects the Y-axis above the origin. In addition, multi-subunit enzymes do not always display cooperativity (see chapter 8) (15).

Possible physical interpretations of the action of TBA^+ and $TPeA^+$

If the large TAA^+ cations enter the conduction pathway of the ryanodine receptor-channel, how might they cause partial block? A form of partial block has been observed in ion channels which are believed to be composed of multibarrelled pores which gate in a coordinated fashion (16, 17). There are both theoretical and experimental reasons for believing that the ryanodine receptor-channel may consist of a number of coordinated conduction pathways. The maximal conductance of the receptor channel monitored with K^+ as the permeant ion is ~900 pS (12) which is close to twice the theoretical limit achievable by an ion-selective channel (18, 19). This apparent anomaly could be accounted for by the presence of more than one conductance pathway in the functional unit channel. The presence of multiple conductance pathways has also been proposed by authors who observe various subconductance states of the purified ryanodine receptor channel (20).

If TAA^+ block of the ryanodine receptor-channel occurs as the result of the occlusion of individual subconductance pathways then we would expect to see a series of subconductance states, each a fraction of the normal unitary value, rather than the observed single subconductance level. In addition, the conductance of the modified conductance state is different for TBA^+ and $TPeA^+$ which again is inconsistent with block of separate conduction pathways.

The TBA^+ related subconductance state displays similar conduction properties to the unmodified channel (see results). In the presence of the large TAA cations, the reduced conductance state appears to behave as if an additional energy barrier has been placed in front of the normal conduction pathway.

The following could then be a valid physical interpretation of the TAA^+ effect. A significant proportion of the voltage drop across the channel falls over a large mouth region at the cytosolic face of the protein. Electrostatic considerations do suggest that for a short, wide pore a significant proportion of the voltage drop may extend out into a large mouth or vestibule (21–24). TBA^+ and $TPeA^+$ interact with a site at the extremity of the voltage drop. Two or more TBA and TPeA cations come together at this region at a common binding site. The electrostatic repulsion between the positively charged organic cations is stabilized by hydrophobic interaction at this binding site. While not occluding the

channel, the mass of positive charge places an electrostatic barrier in front of any other cation entering the pore. The larger size of $TPeA^+$ means that in the presence of this cation the charges are closer together while simultaneously being stabilized by its greater hydrophobicity. The resulting effect is a larger energy barrier that reduces conductance to a greater extent than TBA^+. In other words the addition of TBA^+ or $TPeA^+$ increases the surface charge around the entrance to the conduction pathway (25) and provides an electrostatic barrier for permeant ion translocation. The relationship of the channel mouth to the surface membrane, in particular whether changes in bilayer surface charge could influence the effect remain to be established. We envisage the mouth region being relatively large and effectively insulated from the surface membrane.

This physical mechanism and accompanying kinetic scheme go some way to providing an explanation for the similarities and differences in the action of TBA^+ and $TPeA^+$.

This work was supported by funds from the Medical Research Council and the British Heart Foundation.

Received for publication 7 October 1991 and in final form 21 January 1992.

REFERENCES

1. Neher, E., and J. H. Steinbach. 1978. Local anaesthetics transiently block currents through single acetylcholine-receptor channels. *J. Physiol. (Lond.)*. 277:153–176.
2. Miller, C. 1982. Bis-quaternary ammonium blockers as structural probes of the sarcoplasmic reticulum K^+ channel. *J. Gen. Physiol.* 79:869–891.
3. Latorre, R. 1986. The large calcium-activated potassium channel. *In* Ion Channel Reconstitution. C. Miller, editor. Plenum Publishing Corp., New York. 431–467.
4. Prod'hom, B., D. Pietrobon, and P. Hess. 1987. Direct measurement of proton transfer rates to a group controlling the dihydropyridine-sensitive Ca^{2+} channel. *Nature (Lond.)*. 329:243–246.
5. Pietrobon, D., B. Prod'hom, and P. Hess. 1989. Interactions of protons with single open L-type calcium channels. pH dependence of proton-induced current fluctuations with Cs^+, K^+ and Na^+ as permeant ions. *J. Gen. Physiol.* 94:1–21.
6. Prod'hom, B., D. Pietrobon, and P. Hess. 1989. Interactions of protons with single open L-type calcium channels. Location of protonation site and dependence of proton-induced current fluctuations on concentration and species of permeant ion. *J. Gen. Physiol.* 94:23–42.
7. Ravindran, A., L. Schild, and E. Moczydlowski. 1991. Divalent cation selectivity for external block of voltage-dependent Na^+ channels prolonged by batrachotoxin. Zn^{2+} induces discrete substates in cardiac Na^+ channels. *J. Gen. Physiol.* 97:89–115.
8. Schild, L., A. Ravindran, and E. Moczydlowski. 1991. Zn^{2+}-induced subconductance events in cardiac Na^+ channels prolonged by batrachotoxin. Current-voltage behavior and single-channel kinetics. *J. Gen. Physiol.* 97:117–142.
9. Lindsay, A. R. G., and A. J. Williams. 1991. Functional characterisation of the ryanodine receptor purified from sheep cardiac muscle sarcoplasmic reticulum. *Biochim. Biophys. Acta.* 1064:89–102.
10. Miller, C. 1982. Open-state substructure of single chloride channels from *Torpedo* electroplax. *Phil. Trans. R. Soc. Lond. B.* 299:401–411.
11. Colquhoun, D., and F. J. Sigworth. 1983. Fitting and statistical analysis of single-channel recording. *In* Single-channel Recording. B. Sakmann and E. Neher, editors. Plenum Publishing Corp., New York. 191–263.
12. Lindsay, A. R. G., S. D. Manning, and A. J. Williams. 1991. Monovalent cation conductance in the ryanodine receptor channel of sheep cardiac muscle sarcoplasmic reticulum. *J. Physiol. (Lond.)*. 439:463–480.
13. Woodhull, A. M. 1973. Ionic blockage of sodium channels in nerve. *J. Gen. Physiol.* 61:687–708.
14. Strecker, G. J., and M. B. Jackson. 1989. Curare binding and the curare-induced subconductance state of the acetylcholine receptor channel. *Biophys. J.* 56:795–806.
15. Fersht, A. 1977. Enzyme structure and mechanism. Freeman Publications, San Francisco.
16. Matsuda, H., H. Matsuura, and A. Noma. 1989. Triple-barrel structure of inwardly rectifying K^+ channels revealed by Cs^+ and Rb^+ block in guinea-pig heart cells. *J. Physiol. (Lond.)*. 413:139–157.
17. Miller, C., and M. W. White. 1984. Dimeric structure of single chloride channels from *Torpedo* electroplax. *Proc. Natl. Acad. Sci. USA.* 81:2772–2775.
18. Lauger, P., 1976. Diffusion-limited ion flow through pores. *Biochim. Biophys. Acta.* 455:493–509.
19. Hille, B. 1984. Ionic channels of excitable membranes. Sinauer, Sunderland, MA.
20. Liu, Q-Y., F. A. Lai, E. Rousseau, R. V. Jones, and G. Meissner. 1989. Multiple conductance states of the purified calcium release channel complex from skeletal sarcoplasmic reticulum. *Biophys. J.* 55:415–424.
21. Latorre, R., and C. Miller. 1983. Conduction and selectivity in potassium channels. *J. Membr. Biol.* 71:11–30.
22. Jordan, P. C. 1984. Effect of pore structure on energy barriers and applied voltage profiles. I. Symmetrical channels. *Biophys. J.* 45:1091–1100.
23. Jordan, P. C. 1984. Effects of pore structure on energy barriers and applied voltage profiles. II. Unsymmetrical channels. *Biophys. J.* 45:1101–1107.
24. Yellen, G. 1987. Permeation in potassium channels: Implications for channel structure. *Annu. Rev. Biophys. Biophys. Chem.* 16:227–246.
25. Green, W. N., and O. S. Andersen. 1991. Surface charges and ion channel function. *Annu. Rev. Physiol.* 53:341–359.